(1983) *Biochim. Biophys. Acta 732*, 282.
Tu, A. T. (1982) *Rattlesnake Venoms: Their Actions and Treatment*, p 303, Marcel Dekker, New York.
Tu, A. T., & Morita, M. (1983) *Br. J. Exp. Pathol. 64*, 633.
Verma, P., & Wallach, D. F. H. (1976) *Biochim. Biophys. Acta 426*, 616.
Warren, G. B., Houslay, M. D., Metcalfe, J. C., & Birdsall, N. J. M. (1975) *Nature (London) 255*, 684.

Influence of Trinitrophenylation on the Structure and Dynamics of Phosphatidylethanolamine-Containing Model Membranes

Gert van Duijn,* Jan Dekker, José Leunissen-Bijvelt, Arie J. Verkleij, and Ben de Kruijff
Institute of Molecular Biology, State University of Utrecht, Transitorium 3, Padualaan 8, 3584 CH Utrecht, The Netherlands
Received February 22, 1985; Revised Manuscript Received June 28, 1985

ABSTRACT: The influence of trinitrophenylation on hydration, acyl chain melting characteristics, and polymorphism of phosphatidylethanolamine- (PE-) containing model membranes has been investigated. ^2H nuclear magnetic resonance spectroscopy (NMR) was used to study the hydration properties of (trinitrophenyl)phosphatidylethanolamine (TNPPE). ^{31}P NMR techniques, including saturation transfer and the use of phosphatidylcholine thio analogues, were employed to investigate the TNPPE head-group conformation. The thermotropic behavior of PE/TNPPE mixtures was studied by means of differential scanning calorimetry. The macroscopic organization of the phospholipids was monitored by ^{31}P NMR, small-angle X-ray diffraction, and freeze–fracture electron microscopy. The results indicate that TNPPE is anhydrous in character and does not form ordered structures by itself. Furthermore, even in excess of water, the phosphate region of the fluid TNPPE molecules cannot undergo long-axis rotation, presumably due to intermolecular ring interactions. On the other hand, in aqueous dispersions TNPPE molecules are to a limited extent ($\simeq$20 mol %) soluble in PE. From the decrease in enthalpy of the gel to liquid-crystalline phase transition the TNPPE molecules appear to interact with PE molecules in a 1:4 stoichiometry. In hydrated mixtures with phosphatidylcholine (PC) or PE, the phosphate moiety of the TNPPE molecule undergoes long-axis rotation. However, by comparison with PC and PE in these samples, TNPPE has a different head-group conformation. This is possibly caused by a trinitrophenyl ring orientation either at the bilayer/water interface or perpendicular to the plane of the bilayer. TNPPE hardly influences the temperature of the gel to liquid-crystalline phase transition in PE bilayers. In contrast, TNPPE strongly destabilizes the bilayer organization in both PE and PC model membranes, most likely due to dehydration effects and interbilayer trinitrophenyl ring interactions.

During the last decade the polymorphism of various phospholipid classes has been studied intensively [for a recent review, see De Kruijff et al. (1984)]. PE[1] is probably the best studied phospholipid that can undergo a reversible transition from bilayer to hexagonal (H_{II}) phase (Luzzati et al., 1966; Cullis & De Kruijff, 1978; Rand et al., 1971; Seddon et al., 1983, 1984). The suggestion that nonbilayer phospholipid structures are involved in physiologically important events has been made since the discovery of lipid polymorphism (Luzzati, 1968; Lucy, 1964; Shipley, 1973). There are several indirect arguments to suggest that transiently occurring nonlamellar lipid structures or hexagonal (H_{II}) phase prefering phospholipids, by the nature of their low head-group hydration, could play an important role in membrane function. For instance, the ^{31}P NMR characteristics of rabbit and rat liver microsomes (Stier et al., 1978; De Kruijff et al., 1980c) and the phase preference of the isolated endogenous PE (De Kruijff et al., 1980c) suggest that nonbilayer phospholipid phases might occur in this membrane and that these are possibly related to functional properties of the microsomal membrane like, e.g., membrane fusion and the transmembrane movement of phospholipids.

One approach in investigating the possible biological importance of PE polymorphism is to study the structural and functional aspects of PE head-group modifications in membranes. The best known and most convenient probe to modify and detect aminophospholipids is TNBS (Litman, 1974, 1975; Higgins & Pigott, 1982; Sleight & Pagano, 1983; Hoekstra & Martin, 1982), which reacts with PE under the formation of a trinitrophenyl derivative (structure **1**). A prerequisite for such an approach is to know whether TNBS labeling affects the physical properties of PE. As a first step in this direction, we investigated the effects of TNBS labeling on acyl-chain melting characteristics, hydration, and polymorphism of model membranes composed of PE, mixtures of PC and PE, and microsomal lipids, respectively, by using ^{31}P NMR, DSC, SAXS, and freeze–fracture electron microscopy. It will be shown that PE and TNPPE show a drastically

[1] Abbreviations: PE, phosphatidylethanolamine; DOPE, 1,2-dioleoyl-*sn*-glycero-3-phosphoethanolamine; DOPC, 1,2-dioleoyl-*sn*-glycero-3-phosphocholine; PC, phosphatidylcholine; NMR, nuclear magnetic resonance; DPPE, 1,2-dipalmitoyl-*sn*-glycero-3-phosphoethanolamine; TNBS, trinitrobenzenesulfonic acid; DSC, differential scanning calorimetry; TNPPE, (trinitrophenyl)phosphatidylethanolamine; DEPE, 1,2-dielaidoyl-*sn*-glycero-3-phosphoethanolamine; DEPC, 1,2-dielaidoyl-*sn*-glycero-3-phosphocholine; HPTLC, high-performance thin-layer chromatography; Pipes, 1,4-piperazinediethanesulfonic acid; SAXS, small-angle X-ray scattering; DETNPPE, 1,2-dielaidoyl-*sn*-glycero-3-[(trinitrophenyl)phosphoethanolamine]; DOTNPPE, 1,2-dioleoyl-*sn*-glycero-3-[(trinitrophenyl)phosphoethanolamine]; $\Delta\sigma$, residual chemical shift anisotropy.

0006-2960/85/0424-7640$01.50/0

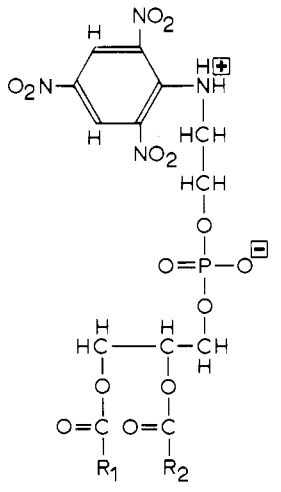

1

different phase behavior. The differences will be discussed in relation to head-group hydration and the shape–structure concept.

Materials and Methods

Purification and Synthesis of Phospholipids. Egg PC and egg PE were purified as described recently (Van Duijn et al., 1984). 1,2-Dioleoyl-*sn*-glycero-3-phosphoethanolamine (DOPE) and 1,2-dielaidoyl-*sn*-glycero-3-phosphoethanolamine (DEPE) were synthesized from DOPC and DEPC, respectively, with phospholipase D (from Brussels sprouts) in the presence of ethanolamine according to Comfurius & Zwaal (1979). DOPC and DEPC were prepared according to the procedure of Van Deenen & De Haas (1964).

The trinitrophenyl derivatives of different PE's (TNPPE) were synthesized according to Siakotos (1967) with the modification that 100 μmol of PE was first dissolved in 6 mL of $CHCl_3$. To this solution was added 12 mL of CH_3OH containing 500 μmol of TNBS. The reaction was started by adding 2 mL of 25% NH_3 at 25 °C. After 2 h the phospholipids were extracted from this reaction medium according to the method of Bligh & Dyer (1959). The lipid extract was evaporated under reduced pressure, and the residual lipids were dissolved in 5 mL of $CHCl_3$. The byproduct of this reaction, trinitroaniline, was removed via adsorption chromatography on a silica column in $CHCl_3$. The TNPPE was eluted in $CHCl_3$/MeOH (1:1 by volume) and was stored in $CHCl_3$ at −20 °C as a stock solution of approximately 10 mM as determined by the method of Böttcher et al. (1961). 1,2-Diacyl-*sn*-glycero-3-thiophosphocholine was synthesized from egg PC in the following steps: (1) Egg PC (800 μmol) was dissolved in 100 mL of diethyl ether. After addition of 98 mL of buffer (5 mM $CaCl_2$, 100 mM Tris, pH 7.4) and 2 mL of glycerol, containing 35 IU of phospholipase C (from *Clostridium welchii*), the reaction mixture was shaken vigorously at 37 °C for 2 h. After separation of the two phases, the diethyl ether fraction, containing the diacylglycerol, was evaporated to dryness. (2) The diacylglycerol was converted to the diacyl-*sn*-glycero-3-thiophosphoric acid bromoethyl ester essentially according to the method of Eibl (1980), except that $POCl_3$ was replaced by $PSCl_3$. (3) Egg thiophosphatidylcholine was synthesized from the bromoethyl ester according to Diembeck & Eibl (1979). Finally, the thio analogue of egg PC was purified by means of partition chromatography on silica gel with $CHCl_3$/MeOH/NH_3/H_2O (30:70:2:2 by volume) as the eluent. It can be expected that the final egg thiophosphatidylcholine is a mixture of two diastereomers (Jiang et al., 1984). The chemical shift of the ^{31}P NMR resonance of the pure thiophosphatidylcholine dissolved in $CDCl_3$ was −56.8 ppm from H_3PO_4, in agreement with the data of Vasilenko et al. (1982). The final yield was 13%.

Total lipid extract of rat liver microsomes was obtained by the method of Folch et al. (1957). Microsomes from adult male Wistar rats were prepared according to Dallner (1974). Microsomal phospholipids were separated by two-dimensional thin-layer chromatography according to Broekhuyse (1969). All lipids were pure as judged by thin-layer chromatography using HPTLC plates with $CHCl_3$/MeOH/NH_3/H_2O (68:28:2:2 by volume) as the eluent.

Liposome Preparation. Lipids, mixed at the desired ratio in chloroform, were dried by evaporation under reduced pressure. Residual solvent was removed under high vacuum over 16 h. The lipids were dispersed by vortexing in a buffer (25% ^2H_2O) containing 100 mM NaCl and 10 mM Pipes/NaOH (pH 7.0). For deuterium NMR experiments, lipid samples partially hydrated with ^2H_2O were prepared according to Ulmius et al. (1977).

The trinitrophenylation of aminophospholipids in aqueous dispersions was performed according to a modified method of Rothman & Kennedy (1977). In short, to a lipid dispersion (approximately 75 mM in 1 mL of 170 mM $NaHCO_3$ buffer, pH 7.8) 10 mL of a 20 mM TNBS solution in 5% $NaHCO_3$ (pH 8.0) was added. After an incubation of 1 h at 25 °C, the hydrated lipids were centrifuged (20000*g*, 20 min; 4 °C), and the pellet was washed 2 times with 170 mM $NaHCO_3$ buffer (pH 7.8).

X-ray Diffraction. Small-angle X-ray diffraction was performed at different temperatures on a Kratky camera with a 10 × 0.2 mm Cu K_α beam (40 kV, 20 mA) equipped with a position-sensitive detector (LETI). An entrance slit of 100 μm was used. The aqueous lipid samples were mounted in slits (12 × 2 × 2 mm) in between two sheets of cellophane. The exposure time for each measurement was 5–10 min.

Differential Scanning Calorimetry (DSC). DSC was carried out on a Perkin-Elmer DSC-2 calorimeter as described by Van Dijck et al. (1976). Lipid dispersions, prepared as described above, were centrifuged at 20000*g* (15 min; 4 °C). A part of the pellet was transfered to a 20-μL sample pan. Heating scans were recorded at a scanning rate of 5 °C/min. The enthalpy of both the gel to liquid-crystalline and the bilayer to hexagonal transitions was calculated by integrating the peaks with a Hewlett-Packard digitizer (type 9864A). The main transition of DEPE (ΔH = 6.9 ± 0.1 kcal/mol of DEPE) was used as a reference (De Kruijff et al., 1984). The transition temperature was determined as the intercept between the base line and the tangent of the rising slope.

Freeze–Fracture Electron Microscopy (FFEM). For freeze–fracturing, the samples were quenched at room temperature by one-sided jet-freezing as described by Knoll et al. (1982). No cryoprotectants were used. The frozen samples were subsequently worked up in a Balzer freeze–etch machine according to standard procedures. The replicas were examined in a Philips 301 electron microscope.

Nuclear Magnetic Resonance (NMR). Broad-band proton-decoupled ^{31}P NMR spectra of dry lipid powders were obtained with a Bruker WP200 spectrometer operating at 81 MHz. Free induction decays were accumulated from 5000 to 7000 transients employing a 18-μs 90° radio-frequency pulse, a 50-kHz sweep width, and a 5-s interpulse delay. An exponential multiplication corresponding to 100-Hz line broadening was applied to the accumulated free induction decays prior to Fourier transformation. The dry phospholipid samples were prepared by evaporation of the organic solvent ($CHCl_3$) under reduced pressure. Residual solvent was re-

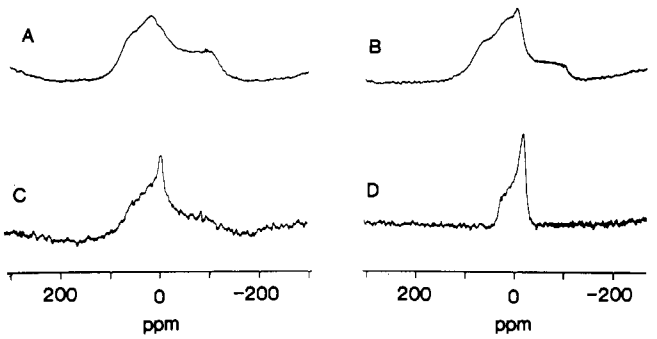

FIGURE 1: Dry powder proton-decoupled 81.0-MHz ^{31}P NMR spectra of egg (trinitrophenyl)phosphatidylethanolamine (A) and DEPE (B). Proton-decoupled 81.0-MHz ^{31}P NMR spectra of egg (trinitrophenyl)phosphatidylethanolamine (C) DEPE (D) in the presence of an excess of buffer. All spectra were recorded at 30 °C.

moved under high vacuum over 16 h. This procedure probably results in the formation of the phospholipid monohydrate.

The 36.4-MHz proton-decoupled (input power 18 W) ^{31}P NMR spectra of aqueous dispersions were recorded on a Bruker WH90 spectrometer as described recently (Van Duijn et al., 1984). Alternatively, proton noise-decoupled ^{31}P NMR spectra of some aqueous lipid samples were recorded at 81 MHz on a Bruker WP200 spectrometer as described by Van Echteld et al. (1981).

^{31}P NMR saturation transfer spectra were obtained at 81 MHz on a Bruker WP200 spectrometer. A peripheral frequency synthesizer (type PTS160) and broad-band radio-frequency modulator (Bruker B-SV3BX; 33-dB attenuation), interfaced to the aspect 2000 computer and pulse programmer, were used for saturation. The selective (CW mode) saturation was gated and on during 1 s. The 18-μs 90° measuring pulse was given 10 μs after the synthesizer was switched off. After data acquisition (sweep width 25 kHz, 4K data points), the synthesizer was switched on again and the sequence was repeated. The spectra was simultaneously gated and broad-band proton-decoupled on a 0.2-W input power level during the selective saturation and on a 3-W input level during the pulse and data acquisition. To avoid time-dependent effects and to obtain reliable control spectra, the entire sequence was repeated 50 times with selective saturation in the spectrum followed by 50 times off resonance (14-kHz downfield). The total number of free induction decays collected per frequency setting was 3000. To increase the signal to noise ratio, the accumulated free induction decays were exponentially multiplied, resulting in a 50-Hz line broadening prior to Fourier transformation.

^{2}H NMR spectra were obtained with a Bruker WP200 spectrometer operating at 30.7 MHz. Free induction decays were accumulated from up to 100 transients by employing a 46-μs 90° radio-frequency pulse, 10-kHz sweep width (4K data points), and 1-s interpulse delay. Spin–lattice relaxation (T_1) measurements were performed by the inversion–recovery method (180°–τ–90°).

Chemicals. Trinitrobenzenesulfonic acid was obtained from Sigma (St. Louis, MO). Thiophosphoryl chloride was purchased from Fluka (Buchs, CH). Chloroform and methanol were distilled before use. Other reagents were of analytical grade.

RESULTS

Characteristics of Pure TNPPE. The ^{31}P NMR dry powder pattern of egg TNPPE, recorded at 30 °C, is shown in Figure 1A. The resonance frequencies of the edges and the peak of this spectrum correspond with the principal elements of a static axially asymmetric tensor, which describes the chemical shift

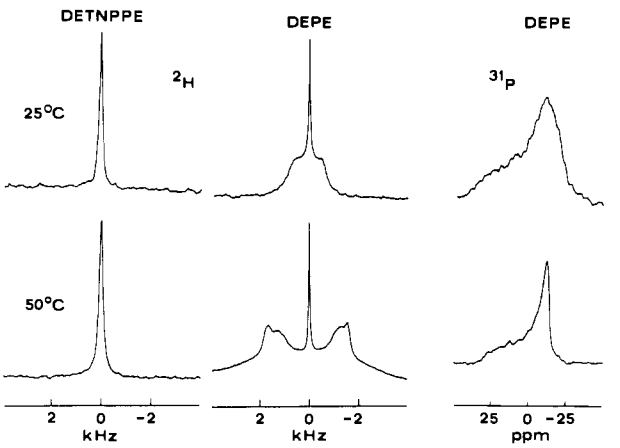

FIGURE 2: The 30.7-MHz ^{2}H NMR spectra of $^{2}H_2O$/DETNPPE and $^{2}H_2O$/DEPE and proton-decoupled 81.0-MHz ^{31}P NMR spectra of DEPE at a temperature below (25 °C) and above (50 °C) the gel to liquid-crystalline phase transition. In both samples, the phospholipid to $^{2}H_2O$ molar ratio is 1:7.

anisotropy. Since these values (77, 23, and −100 ppm) reveal a great similarity with the data obtained by Kohler & Klein (1977) for anhydrous DPPE at 27 °C (81, 20, and −105 ppm), it can be concluded that the electronic distribution around the phosphate and, thereby, the shielding of the ^{31}P nucleus of TNPPE and PE are the same. Since DSC experiments reveal a lipid phase transition for the dry TNPPE at 10 °C, this suggests that the acyl chains are melted at 30 °C. To detect whether for dry PE with fluid acyl chains similar ^{31}P NMR behavior could be observed, the ^{31}P NMR dry powder characteristics of DEPE were recorded at various temperatures. At 30 °C the spectrum was very similar to that of egg TNPPE (Figure 1B). At 50 °C the dry DEPE gives rise to a ^{31}P NMR signal that is typical for a shielding tensor that is axially symmetric ($\Delta\sigma \approx 76$ ppm; data not shown. The concomitant partial averaging of the chemical shift anisotropy is apparently caused by the onset of motion around the long axis of the phospholipid molecule, due to the melting of the acyl chains. Moreover, at 85 °C the ^{31}P NMR spectrum of the dry DEPE, characterized by a reversed asymmetry and a reduced line width, is typical for phospholipids in a hexagonal organization. This interpretation of the ^{31}P NMR data of dry DEPE is consistent with the observation by DSC of a broad transition between 45 and 80 °C (data not shown). Up till 70 °C, these ^{31}P NMR spectral changes are not detectable for the dry trinitrophenyl derivatives of egg PE.

In contrast to DEPE (Figure 1D), the ^{31}P NMR characteristics of egg TNPPE are virtually independent of adding aqueous buffer to the lipid. Only a small (maximally 1% of total signal intensity) isotropic peak is superimposed on the spectrum (Figure 1C). These results suggest that the head group of TNPPE is not hydrated even in an excess of buffer. Furthermore, it can be concluded from these results that the phosphate moiety of the TNPPE molecules cannot undergo long-axis rotation in the liquid-crystalline state. This is possibly due to intermolecular ring–ring stacking of the trinitrophenyl groups. Since SAXS experiments only show a broad scattering profile for egg TNPPE in the presence of water, the TNPPE molecules appear to be present in disordered molecular aggregates. Not surprisingly, FFEM does not show any organized structure in the same sample (data not shown).

In order to gain further insight in the hydration properties of the trinitrophenyl derivative of PE, we performed ^{2}H NMR measurements on both DEPE and DETNPPE in the presence of 7 mol of $^{2}H_2O$/mol of lipid (Figure 2). This molar ratio

Table I: Deuterium T_1 Relaxation Times of DEPE/^2H_2O (1:7), DETNPPE/^2H_2O (1:7), and ^2H_2O[a]

	T_1 (ms)	
	25 °C	50 °C
DEPE (isotropic)	270 ± 10	410 ± 10
DEPE	35 ● 5	75 ± 5
DETNPPE	240 ± 10	230 ± 20
^2H_2O	417	645

[a] The data for DEPE represent the T_1 measurements for the spectrum giving rise to a quadrupolar splitting. The T_1 is similar for both quadrupolar splittings observed at 50 °C.

was chosen because under these conditions a portion of the ^2H_2O molecules undergoes restricted motion. This is due to binding to the PE head group as has been reported by Borle & Seelig (1983) for PE from *Escherichia coli* cells. For DEPE in the gel state (for a comparison, see ^2H NMR and ^{31}P NMR spectra in Figure 2) at 25 °C, a considerable portion (85%) of the ^2H_2O molecules undergoes restricted and axially symmetric motion resulting in a quadrupole splitting ($\Delta\nu_q$) of 1.2 kHz. The remainder of the ^2H_2O molecules undergo isotropic motion and do not rapidly exchange with the lipid-bound fraction. In the liquid-crystalline state (50 °C) of DEPE, two quadrupolar splittings are observed with $\Delta\nu_q$ values of 2.8 and 3.5 kHz. The increase of the quadrupolar splitting in the liquid-crystalline state seems controversial since one would expect a more rapid motion of the lipid-bound ^2H_2O molecules resulting in a decreased quadrupole splitting. However, the observed ^2H NMR spectra can be understood in terms of a three water pools model (Söderman et al., 1983). One pool consists of water molecules that are firmly bound to various sites at the head group (primary hydration shell) and that undergo restricted motion. The second pool consists of water molecules that are more loosely associated with the head group but that are also in rapid exchange with the water molecules in the primary hydration shell. Finally, in a third pool the free moving unbound water molecules cannot exchange with the water molecules present in the other two pools. Apparently, in the gel state of DEPE there are fewer water molecules bound in the primary hydration shell and relatively more loosely associated water molecules. However, these latter water molecules are in rapid exchange with the bound water, leading to a decreasing quadrupole splitting.

On the contrary, in the DETNPPE/^2H_2O sample all the ^2H_2O molecules appear to undergo isotropic motion (line width at half-height ($\Delta\nu_{1/2}$) = 130 Hz) on the NMR time scale both at 25 and at 50 °C (Figure 2), suggesting extremely limited binding to the TNPPE head group. Spin–lattice relaxation measurements confirm the lack of hydration of DETNPPE. For the DEPE sample, the T_1 of the ^2H_2O molecules, which gives rise to a quadrupolar splitting, is greatly reduced compared to the T_1 of the isotropic component in this sample and in pure ^2H_2O (Table I). This demonstrates a reduction in motion of the head group bound ^2H_2O molecules in agreement

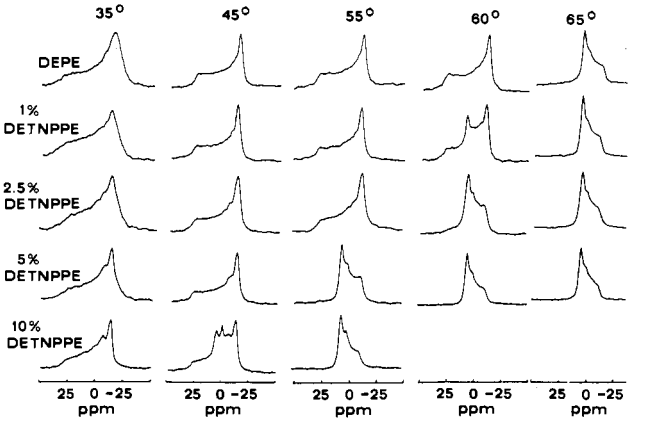

FIGURE 3: Temperature dependency of the proton-decoupled 36.4-MHz ^{31}P NMR spectra obtained from aqueous dispersions of DEPE as a function of DETNPPE incorporation.

with previously published data (Borle & Seelig, 1983). In the case of DETNPPE, the reduction in T_1 is considerably less, demonstrating more rapid motion of ^2H_2O, compared to the PE head group bound ^2H_2O molecules.

DEPE/DETNPPE Mixtures. Figure 3 shows the ^{31}P NMR spectra of aqueous dispersions of DEPE with increasing amounts of DETNPPE incorporated. In agreement with previous data and detailed discussions (Cullis et al., 1976; Cullis & De Kruijff, 1976), for fully hydrated DEPE both the gel to liquid-crystalline (around 35 °C) and the bilayer to hexagonal (H_{II}) phase transition (around 65 °C) show up in the ^{31}P NMR spectra as a decrease in line width and a change in sign and magnitude of the chemical shift anisotropy, respectively.

Incorporation of up to 10 mol % of DETNPPE in DEPE results in a decrease of the bilayer to hexagonal (H_{II}) phase transition temperature, while no effect is detectable for the gel to liquid-crystalline transition temperature. In addition, in the 10 mol % DETNPPE-containing sample at 45 °C, a small isotropic signal, as well as a new resonance peak, appears in this spectrum at −5.0 ppm. This resonance peak, which is clearly a result of the incorporation of DETNPPE, has been investigated and will be discussed in detail in subsequent sections. At higher DETNPPE concentrations a more complex ^{31}P NMR behavior was observed, including the appearance of broad isotropic signals (data not shown).

The data from the small-angle X-ray diffraction experiments are consistent with the ^{31}P NMR results and are shown in Figure 4 and Table II. For DEPE, one diffraction band is present up to 55 °C. We suggest that this represents the first-order reflection of a lamellar phase. Between 35 and 40 °C the interbilayer repeat distance reduces from 65.1 to 55.0 Å due to the transition from the gel state to the liquid-crystalline state. At 65 °C, three diffraction bands show up with a $1:1/\sqrt{3}:1/_2$ distance relationship, indicative of a hexagonal organization. The corresponding tube to tube distance is

Table II: Repeat Distances (Å) in L_β and L_α Phases and, in Parentheses, Tube Diameters (Å) in Hexagonal (H_{II}) Phases of Hydrated DEPE/DTNPPE Mixtures as a Function of Temperature[a]

mol % DETNPPE in DEPE	25 °C	35 °C	40 °C	45 °C	50 °C	55 °C	60 °C	65 °C
0	65.1	65.1	55.0	53.8	53.5	53.1	52.4 (75.8)	(73.9)
1	65.1	64.0	55.0	53.8	53.5	52.8	51.7 (75.1)	(72.7)
2.5	65.1	63.0	55.0	53.8	53.5	52.4 (75.8)	51.0 (73.9)	(72.1)
10	65.1	58.3	53.8	52.8 (73.9)	52.1 (72.7)	52.8 (70.5)	52.4 (68.3)	52.8 (67.3)
30	65.1	57.4	53.5	56.6 (72.7)	(71.6)	(68.3)	(65.8)	(61.8)
50	65.1	(67.3)	(70.5)	(67.8)	(66.3)	(63.5)	(58.9)	(56.4)

[a] The tube diameter was calculated from the first-order repeat distance times $2/3^{1/2}$.

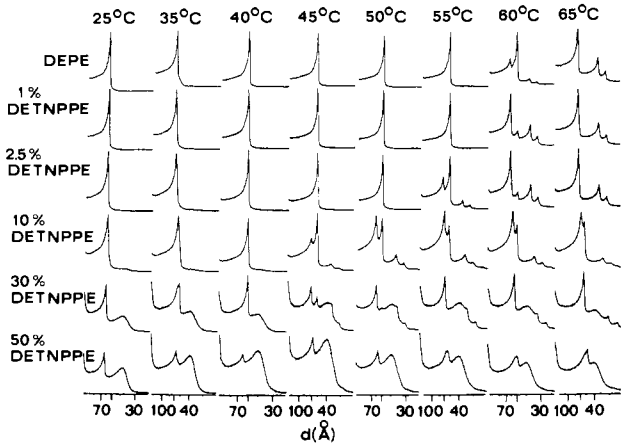

FIGURE 4: Small-angle X-ray diffraction profiles of fully hydrated DEPE with increasing amounts of DETNPPE incorporated as a function of temperature.

expressed in Table II (73.9 Å).

Up till 10 mol %, DETNPPE clearly decreases the bilayer to hexagonal (H_{II}) phase transition temperature of DEPE, while the gel to liquid-crystalline transition temperature appears to be unaffected. However, above 10 mol % the interbilayer repeat distances suggest that the lipids are already in the liquid-crystalline state at 35 °C, suggesting a slight fluidizing effect of DETNPPE in agreement with the forthcoming DSC data (see subsequent section). At higher concentrations of DETNPPE, the X-ray diffraction patterns become more complicated. The sharp diffraction bands are obscured by the appearance of a broad scattering profile, which becomes more dominant with increasing amounts of DETNPPE and which is very similar to that observed for pure DETNPPE in buffer. Probably these broad scattering bands reflect unordered DETNPPE-rich domains that are segregated from a relatively ordered phase, which is DEPE-rich and DETNPPE-poor.

Table III: Differential Scanning Calorimetry Measurements of the L_β–L_α and the L_α–H_{II} Phase Transition Temperatures of Hydrated Mixtures Containing DEPE and Increasing Amounts of DETNPPE

mol % DETNPPE in DEPE	T_x (L_β–L_α) (°C)	ΔT (0.5 h) (L_β–L_α) (°C)	T_x (L_α–H_{II}) (°C)
0	36	2.8	63
1	36	2.5	62
2.5	34	3.0	59
5	33	3.5	53
10	29	5.5	44
20	26	7.0	37
30	29	5.5	39
50	28	6.0	40

DETNPPE does not influence the lamellar repeat distance both in the gel and in the liquid-crystalline state (Table II). On the contrary, the tube diameter in the hexagonal (H_{II}) phase decreases as a result of DETNPPE incorporation. As an example, at 60 °C the tube to tube distance decreases from 75.8 Å in pure DEPE to 58.9 Å in a sample comprised of DEPE and DETNPPE in a 1:1 molar ratio. A considerable part of this effect is due to the strong decrease in tube diameter of hexagonally organized PE's with increasing temperature (Seddon et al., 1984). However, to a limited extent the repeat distance also appears to decrease as a result of DETNPPE incorporation. This can be seen from the tube diameter observed just above the relevant bilayer to hexagonal (H_{II}) phase transition temperature.

The thermotropic behaviors of the DEPE–DETNPPE mixtures are further illustrated in the DSC experiments reported in Figure 5 and Table III. Incorporation of DETNPPE slightly decreases the gel to liquid–crystalline phase transition temperature, which is mainly due to a broadening of the transition. This effect is most apparent in samples containing

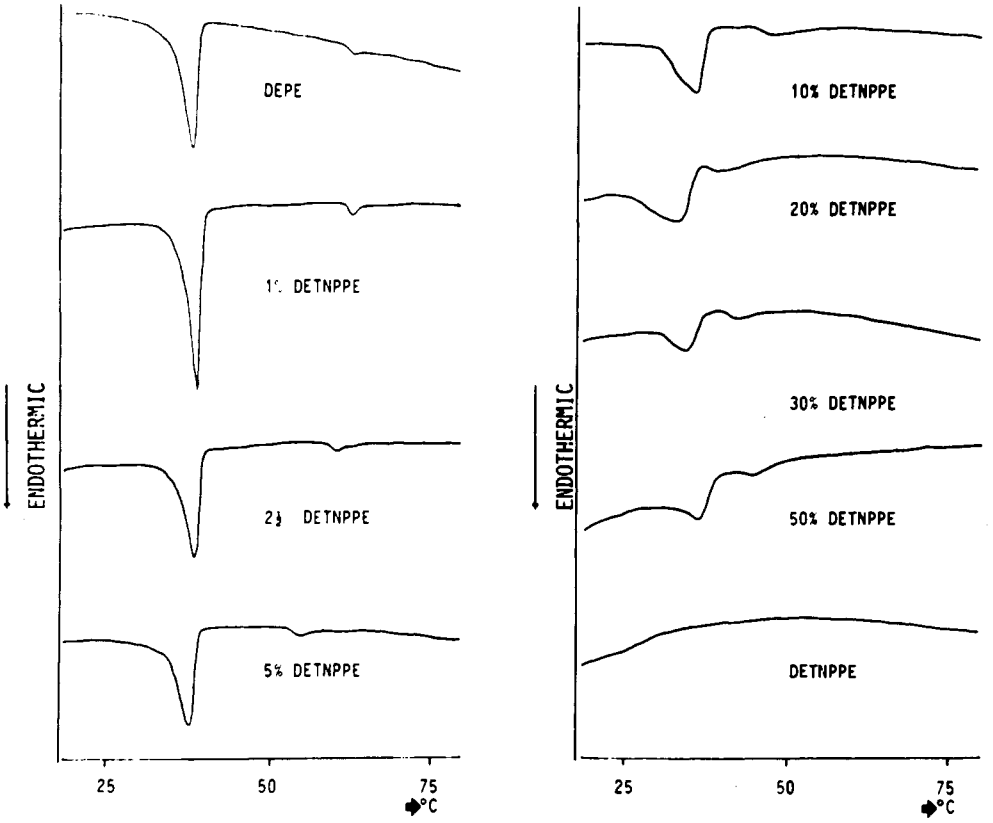

FIGURE 5: DSC heating curves of hydrated mixtures comprised of DEPE and DETNPPE.

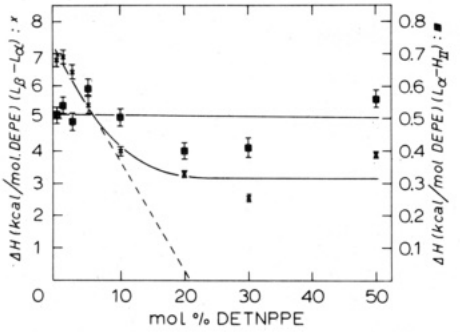

FIGURE 6: DETNPPE concentration-dependent enthalpy changes (ΔH) of DEPE for the gel to liquid-crystalline transition (×) and the bilayer to hexagonal (H_{II}) phase transition (■). The error bars indicate the standard deviations.

more than 5 mol % DETNPPE. In the presence of aqueous buffer, pure DETNPPE does not show any phase transition between 20 and 75 °C. DETNPPE incorporation strongly influences the enthalpy of the gel to liquid–crystalline transition. The ΔH values decrease linearly from 7.0 kcal/mol of DEPE in pure DEPE to about 4.0 kcal/mol of DEPE after incorporation of up to 10 mol % DETNPPE (Figure 6). (It should be emphasized that the ΔH values are expressed per mole of DEPE). In fully hydrated samples containing more than 20 mol % DETNPPE, the enthalpy of the main transition reaches a level of 3.2 kcal/mol of DEPE. This inordinately low transition enthalpy further emphasizes the limited solubility of DETNPPE in DEPE bilayers. In addition, extrapolation of the first linear part of the enthalpy vs. concentration curve (Figure 6) indicates a 1–4 molar interaction between DETNPPE and DEPE.

The decrease in bilayer to hexagonal (H_{II}) phase transition temperature upon DETNPPE incorporation, observed in these calorimetric experiments (Figure 5 and Table III), is in good agreement with the ^{31}P NMR and X-ray data. The enthalpy of the bilayer to hexagonal (H_{II}) phase transition of DEPE is hardly affected by the incorporation of DETNPPE.

DOPC/DOPE/DOTNPPE Mixtures. From the former results presented in this paper it can be concluded that the trinitrophenyl derivative of PE destabilizes the bilayer organization in hydrated mixtures with PE. However, one could question whether this effect is restricted to systems containing PE. In order to answer this question, we investigated the temperature-dependent phase behavior of hydrated DOPC/DOPE mixtures in which DOPE was gradually replaced by DOTNPPE.

Figure 7A demonstrates the ^{31}P NMR characteristics of a DOPC/DOPE (1:4) system, as recorded between 10 and 70 °C. In agreement with the data of Tilcock et al. (1982), up to 30 °C all the lipid molecules give rise to a ^{31}P NMR signal that is typical for a lamellar phase. Freeze–fracture electron microscopy supports this phase behavior, since after quenching the samples from 25 °C only large stacked bilayers are observed (Figure 8a). Above 50 °C the ^{31}P NMR spectra of this sample show isotropic signals, which indicate an averaging of the chemical shift anisotropy due to the rapid motion ($\tau_c < 10^{-5}$ s) of the lipid molecules. The profound hysteresis, as shown by ^{31}P NMR after cooling the sample from 70 to 10 °C (Figure 7A), suggests changes in macroscopic order, e.g., rearrangements involving lipidic particles or cubic phases (Hui et al., 1981).

Replacement of 25% of the DOPE in this sample by DOTNPPE results in dramatic changes in the macroscopic organization of the lipids. As measured by ^{31}P NMR (Figure 7B), most of the lipid molecules undergo isotropic motion at

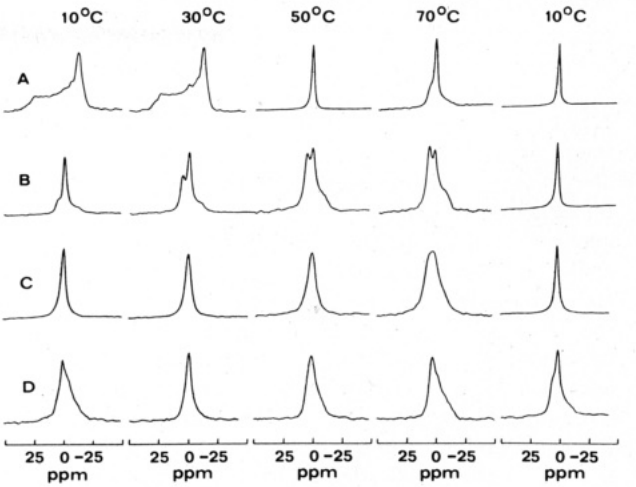

FIGURE 7: Proton-decoupled 36.4-MHz ^{31}P NMR spectra obtained from aqueous dispersions of DOPC/DOPE (1:4) (A), DOPC/DOPE/DOTNPPE (1:3:1) (B), DOPC/DOPE/DOTNPPE (1:2:2) (C), DOPC/DOTNPPE (1:4) (D) at 10, 30, 50, 70, and 10 °C, successively.

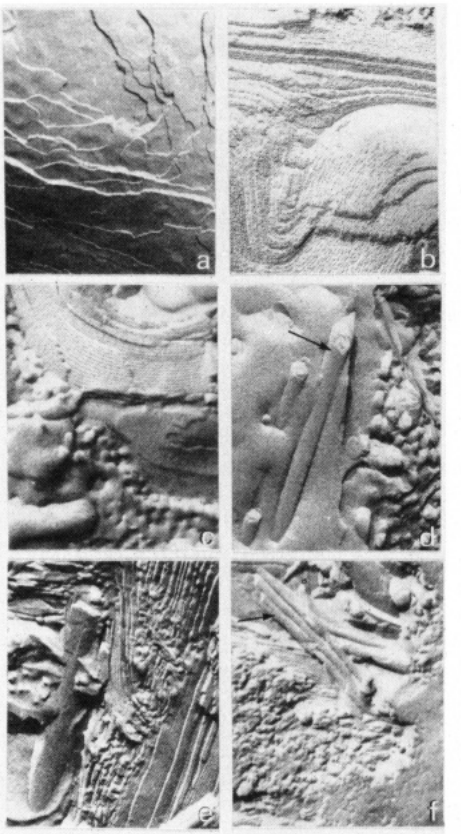

FIGURE 8: Freeze–fracture electron microscopy pictures of hydrated samples consisting of DOPC/DOPE (1:4) (a), DOPC/DOPE/DOTNPPE (1:3:1) (b), DOPC/DOPE/DOTNPPE (1:2:2) (c and d), and DOPC/DOTNPPE (1:4) (e and f). All samples were quenched from room temperature. Magnification 62000×.

10 °C. Moreover, during heating of sample up to 70 °C, the phospholipids tend to organize themselves in a hexagonal (H_{II}) phase, while the contribution of the isotropic component in the spectrum decreases. The bilayer-destabilizing action of DOTNPPE is clearly visualized by comparing the ^{31}P NMR spectra at 30 °C. Freeze-fracture replicas also clearly show the hexagonally organized tubes of this sample when quenched from room temperature (Figure 8b).

Systems containing higher amounts of DOTNPPE give rise to more complicated ^{31}P NMR characteristics. As an example,

the ^{31}P NMR spectra obtained from a hydrated sample consisting of DOPC/DOPE/DOTNPPE (1:2:2) are represented in Figure 7C. Over a temperature range between 10 and 70 °C, the lipids in this sample are responsible for isotropic ^{31}P NMR signals. Assuming that the averaging of the chemical shift anisotropy is due to rapid motion of the lipid molecules, one would expect a narrowing of the line shape upon increasing the temperature. However, as can be seen in Figure 7C, the opposite is true. Possibly, with increasing temperatures, the lipids reorganize into structures in which the molecules undergo a more restricted motion. Freeze–fracture electron microscopy reinforces the complex nature of the phase preference in this lipid mixture. Figure 8c shows the coexistence of bilayer and hexagonal (H_{II}) phases together with intermediate structures such as lipidic particles in this sample when quenched from 25 °C. Besides, as can be seen in Figure 8d (see arrow), bilayers rolled up in so-called cochleated structures are present.

A similar complex polymorphic phase behavior was observed in a system in which no DOPE but only DOTNPPE was present. Figure 7D shows the ^{31}P NMR spectra of a hydrated sample comprised of DOPC/DOTNPPE (1:4), as recorded between 10 and 70 °C. Although an unambiguous structural interpretation is hampered by the appearance of isotropic signals, the line shape of the spectrum derived from this sample at 70 °C, clearly demonstrates a hexagonal organization of the lipids, even in the absence of unmodified DOPE. This bilayer destabilizing effect of DOTNPPE in mixtures with DOPC can be visualized already at 25 °C with freeze–fracture electron microscopy. Figure 8e shows the coexistence of lamellar, hexagonal (H_{II}) phase and other nonlamellar phospholipid structures while in Figure 8f (see arrow) thick tubes are visible.

The next objective in this study was to address the question as to whether lower concentrations of the trinitrophenyl derivative of PE are sufficient to induce nonlamellar phases in PC bilayers. This question is especially relevant in relation to PC:PE ratios found in biological membranes. Since in rat liver microsomes PC and PE represent 60 and 25°, respectively, of the phospholipids (Depierre & Dallner, 1975), we investigated the temperature-dependent phase behavior of a hydrated sample comprised of DOPC/DOTNPPE (7:3) by using ^{31}P NMR and freeze–fracture electron microscopy. As registered by ^{31}P NMR (Figure 9), up to 70 °C no hexagonal (H_{II}) phase can be observed. However, the spectra reveal a sharp isotropic component that is superimposed on a bilayer type of spectrum and becomes more dominant at higher temperatures. Also after the aqueous lipid sample is cooled from 70 to 10 °C, the isotropic peak is still present in the spectrum. This "isotropic phase", which shows a profound hysteresis, possibly represents stable changes in the macroscopic organization of the lipids. Indeed, as illustrated in Figure 10, freeze–fracture electron microscopy confirms this suggestion since not only bilayers but also both randomly arranged (Figure 10a) and more closely packed (Figure 10b) lipidic particles are visible in the hydrated DOPC/DOTNPPE (7:3) mixtures when quenched at room temperature after heating to 70 °C.

Furthermore, the new resonance peak at −5 ppm, which was noticed in the DEPE/DETNPPE system (Figure 3), shows up even more clearly in the ^{31}P NMR spectra of this DOPC/DOTNPPE (7:3) mixture. Besides, up to 50 °C, the line shapes of the spectra in Figure 9 reveal a second low-field shoulder at 10 ppm. The possibility that these signals, induced by TNPPE, represent a bilayer type of spectrum with a reduced line width will be investigated by means of ^{31}P saturation transfer NMR (see later section).

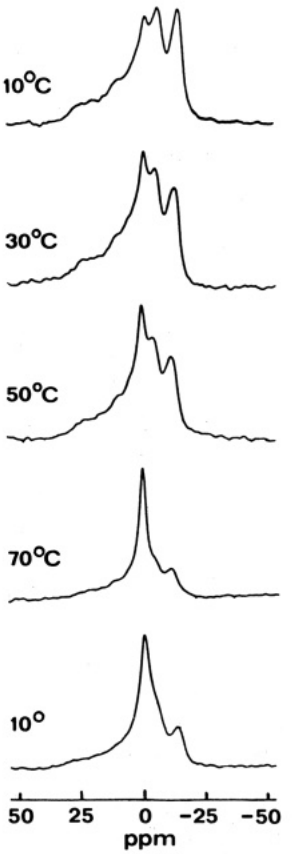

FIGURE 9: Proton-decoupled 36.4-MHz ^{31}P NMR spectra obtained from a fully hydrated mixture of DOPC/DOTNPPE (7:3), recorded at 10, 30, 50, and 70 °C. After heating to 70 °C, the spectrum was recorded again at 10 °C.

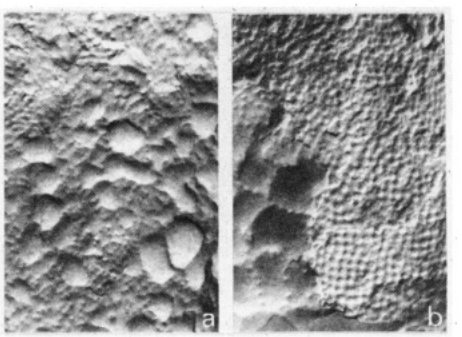

FIGURE 10: Freeze–fracture micrographs of an aqueous dispersion of DOPC/DOTNPPE (7:3), quenched from room temperature after heating to 70 °C. Magnification 39000×.

Microsomal Phospholipids. As there are sufficiently strong indications now that TNPPE's are able to induce nonbilayer structures as well in PE as in PC, we performed some TNBS-modification experiments with lipids extracted from microsomal membranes. In a control experiment (in the absence of TNBS), hydrated lipids derived from rat liver microsomes appear to be organized in bilayers between 10 and 70 °C, as measured by ^{31}P NMR (Figure 11A) and in agreement with previous data (De Kruijff et al., 1978). However, after trinitrophenylation of the aminophospholipid head groups in organic solvents, the hydrated microsomal phospholipids show a dramatically changed temperature-dependent phase behavior, as determined by ^{31}P NMR. First, up to 30 °C, probably all the lipid molecules are organized in bilayers, although a considerable part of the lipids gives rise to a superimposed ^{31}P NMR line shape, which is characterized

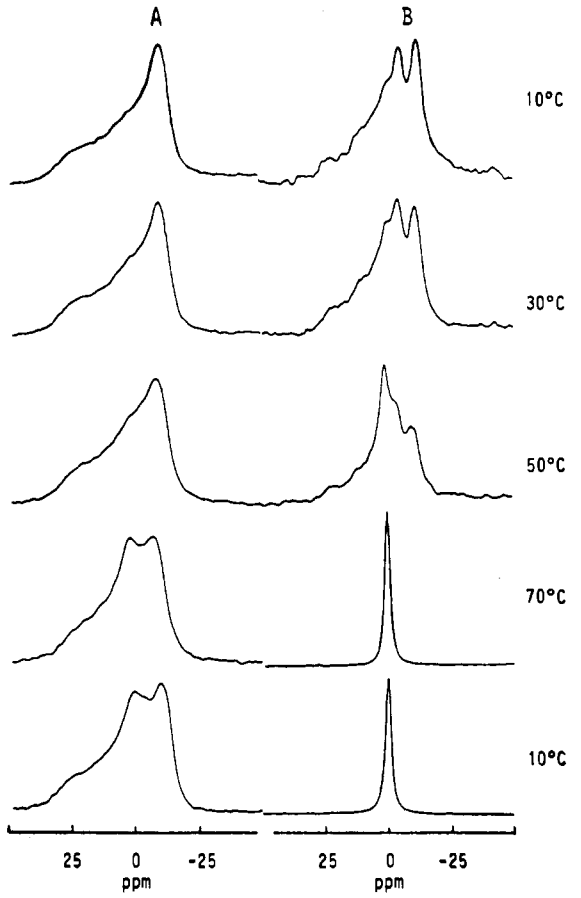

FIGURE 11: Proton-decoupled 36.4-MHz ^{31}P NMR spectra obtained from aqueous dispersions of microsomal phospholipids (A) and of TNBS-modified microsomal phospholipids (B). In the latter sample, no aminophospholipids were present after the trinitrophenylation reaction as judged by thin-layer chromatography. The spectra were recorded at 10, 30, 50, and 70 °C, successively. Finally, the samples were cooled and measured at 10 °C.

by a reduced line width (Figure 11B). Second, up to 70 °C a narrow spectral component becomes increasingly dominant. Although the macroscopic structure of this "isotropic phase" is not known, the observed hysteresis at 10 °C (Figure 11B) strongly suggests a stable macroscopic reorganization of the previous bilayer structure.

Addition of TNBS to aqueous samples comprised of microsomal phospholipids results in a very similar phase behavior. After 1 h of incubation (25 °C) with TNBS (for details, see Materials and Methods), no more unmodified aminophospholipids were present in this system, as judged by two-dimensional thin-layer chromatography (data not shown). Figure 12B shows the 81.0-MHz ^{31}P NMR spectrum, as recorded at 20 °C, of aqueous microsomal phospholipid aggregates in which PE has been trinitrophenylated quantitatively. A comparison between this spectrum and the 81.0-MHz ^{31}P NMR signal obtained from hydrated nonlabeled microsomal phospholipids (Figure 12A) reveals three interesting differences. (1) Due to the higher resolution of the stronger field spectrometer, two distinct high-field peaks at −14 and −12 ppm (derived from PC and PE, respectively) are visible in the ^{31}P NMR bilayer spectrum of hydrated microsomal phospholipids (Figure 12A). Trinitrophenylation of PE clearly leads to the disappearance of the high-field peak at −12 ppm (Figure 12B). (2) As a result of PE head group modification using TNBS, an isotropic signal appears in the ^{31}P NMR spectrum, indicative of lipid molecules undergoing rapid motion ($\tau_c < 10^{-5}$ s). (3) Most interestingly, the presence of TNPPE

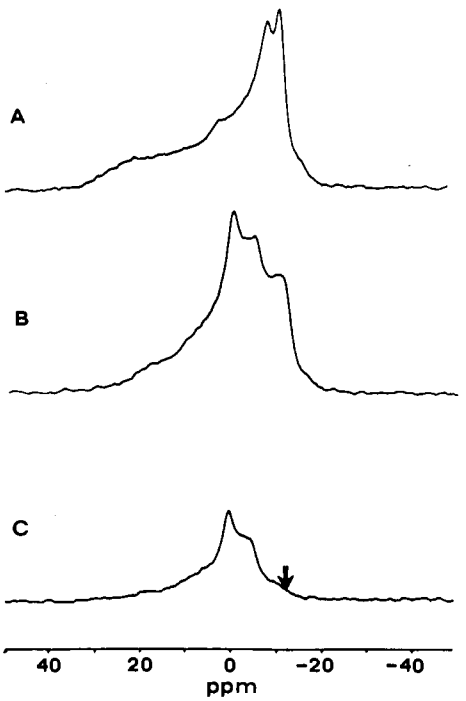

FIGURE 12: Proton-decoupled 81.0-MHz ^{31}P NMR spectra of fully hydrated microsomal phospholipids (A) and of a microsomal phospholipid dispersion after the addition of TNBS (B). (C) As in (B) but with selective saturation at the position indicated by the arrow. (For experimental details, see Materials and Methods.) All spectra were recorded at 20 °C.

in the sample induces a superimposed signal in the ^{31}P NMR spectrum, characterized by a high-field peak at −5.0 ppm and a low-field shoulder at 10 ppm (Figure 12B). These resonance frequency values might correspond with the edges of an axially symmetric powder pattern with a decreased residual chemical shift anisotropy. In order to obtain insight into the nature of this additional part of the spectrum, we performed ^{31}P saturation-transfer NMR measurements according to De Kruijff et al. (1980b). We applied a saturation pulse (1-s) train at the high-field peak of the broad bilayer component of the spectrum (Figure 12B), corresponding with the frequency as indicated by the arrow. This resulted in an elimination of most of the broad bilayer spectrum (Figure 12C). Although a small isotropic component is present, the line shape of the residual spectrum (Figure 12C) rather clearly indicates a bilayer type of spectrum with a high-field peak and a low-field shoulder with, however, an approximately 60% reduced chemical shift anisotropy. Since it has already been concluded that the rigid lattice chemical shift anisotropy in the phosphate region of PE and TNPPE is the same, this reduction of the line width is most likely due to changes in order and/or motion of the phosphate moiety in a part of the lipid molecules in this sample.

Thio-PC/TNPPE Mixture. Although it is evident that the appearance of the second ^{31}P NMR bilayer component is a result of TNPPE incorporation, no direct proof is available that the TNPPE's are themselves organized in this additional phase. The usefulness of thiophospholipids, in which the double-bonded oxygen atom of the phosphate group is replaced by a sulfur atom, in detecting the macroscopic organization of individual lipids in mixed model membranes has been reported by Vasilenko et al. (1982). Figure 13B shows the ^{31}P NMR spectrum, as recorded at 0 °C, of fully hydrated egg thiophosphatidylcholine. In agreement with the data of Vasilenko et al. (1982), this modification results in a ±56 ppm shift of the spectrum to lower field. Figure 13A represents the ^{31}P NMR spectrum obtained from a hydrated mixture

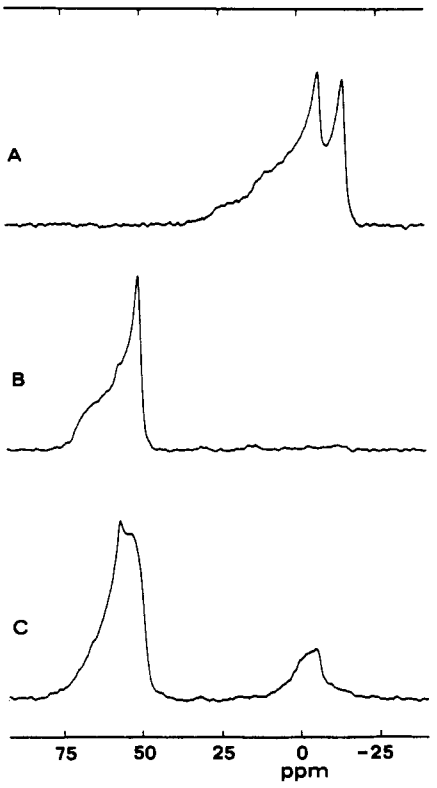

FIGURE 13: The 81.0-MHz ^{31}P NMR spectra of aqueous dispersions of egg PC/DETNPPE (7:3) (A), egg thiophosphatidylcholine (B), and egg thiophosphatidylcholine/DETNPPE (7:3) (C), as recorded at 0 °C.

comprised of egg PC and DETNPPE (7:3). In this spectrum, the two superimposed bilayer components are clearly visible but still indistinguishable on the basis of phospholipid head group. On the contrary, for a hydrated sample consisting of egg thiophosphatidylcholine and DETNPPE (7:3), ^{31}P NMR measurements give rise to two separated (~56 ppm) signals (Figure 13C). The low-field component, representing 70% of the total signal intensity, is derived from the thio analogue of egg PC, while the high-field signal (30% of the total intensity) represents an axially symmetric spectrum with a residual chemical shift anisotropy of 17 ppm, obtained from DETNPPE. This result both reinforces the suggestion that TNPPE's, in hydrated mixtures with other phospholipids, can undergo long-axis rotation and indicates that the phosphate region of TNPPE molecules themselves is responsible for a reduced chemical shift anisotropy, due to changes in local order and/or motion.

Discussion

The purpose of the present study was to investigate the effects of trinitrophenylation on acyl-chain melting characteristics, hydration, and polymorphism of PE-containing model membranes. Dry powder ^{31}P NMR measurements revealed that the electronic environment of the ^{31}P nucleus in TNPPE and PE is the same, since the principle values of the chemical shift anisotropy of egg TNPPE were similar to the data reported by Kohler & Klein (1977) for anhydrous DPPE at 27 °C. However, although DSC data, in agreement with results obtained from a study by Bishop et al. (1979), demonstrated that the acyl chains of egg TNPPE are in the liquid-crystalline state above 10 °C, the dry powder ^{31}P NMR line shape did not change up to 70 °C. On the contrary, melting of the acyl chains in dry DEPE resulted in an axially symmetric ^{31}P NMR line shape with a reduced chemical shift anisotropy ($\Delta\sigma$), which indicates rapid rotation of the phosphate segment around the bilayer normal (Seelig, 1978). Apparently, this long-axis rotation of the phosphate moiety of the TNPPE molecules is prevented in the fluid state, most likely due to intermolecular interaction of the trinitrophenyl groups.

Another interesting property of the trinitrophenyl derivatives of PE is the profoundly anhydrous character of the head group. Addition of aqueous buffer to the TNPPE molecules did not lead to the onset of motion, which would be observed as partial averaging of the chemical shift anisotropy. Furthermore, ^{2}H NMR measurements on the $^{2}H_2O$/phospholipid mixtures revealed that indeed the $^{2}H_2O$–TNPPE interaction is much weaker than the $^{2}H_2O$–PE interaction, emphasizing the overall hydrophobic character of TNPPE. This is also born out by the data of Bishop et al. (1979), who concluded, from monolayer experiments, that the trinitrophenyl groups are oriented at the interface at low surface pressures. In addition, it can be concluded from small-angle X-ray diffraction and freeze–fracture electron microscopy experiments that the TNPPE molecules do not organize themselves into ordered structures even in the presence of water.

On the other hand, when incorporated at low concentrations into the liquid-crystalline phase of PE or PC, TNPPE showed a different organization. In the ^{31}P NMR spectra, a second axially symmetric powder pattern with a small $\Delta\sigma$ of approximately 15 ppm was present and could be shown to originate from the TNPPE molecules themselves. This proves that now the phosphate groups in TNPPE can undergo long-axis rotation. Furthermore, since for naturally occurring membrane phospholipids $\Delta\sigma$ is typically on the order of 40 ppm (Seelig, 1978; Cullis & De Kruijff, 1978) and the rigid lattice spectra of TNPPE and PE are very similar, there must be a different head-group conformation of PE and TNPPE in these systems.

TNPPE clearly reduced the enthalpy (ΔH) of the gel to liquid-crystalline phase transition of PE. This could be the result of an interference by the adjacent bulky TNPPE molecules on the condensation of the PE acyl chains to the gel state. Apparently, the trinitrophenyl derivatives are solubilized in PE bilayers to a limited extent since raising the proportion of TNPPE above 20 mol % did not further decrease the ΔH. Extrapolation to zero of the linear part of the enthalpy vs. TNPPE concentration curve leads to the conclusion that there is a 1:4 stoichiometry between TNPPE and PE and that TNPPE molecules exceeding 20 mol % are segregated in PE-poor domains.

TNPPE molecules also showed a strong influence on the polymorphic phase behavior of hydrated mixtures with PE. The incorporation of up to 10 mol % TNPPE in PE resulted in an almost linear decrease in the bilayer to hexagonal (H_{II}) phase transition temperature. This linearity indicates that in the concentration range between 0 and 10 mol % the TNPPE molecules are distributed homogeneously in aqueous aggregates of PE. Incorporation of more than 10 mol % TNPPE resulted in a more complex phase behavior. ^{31}P NMR spectra revealed the appearance of a superimposed broad isotropic signal, which became more dominant with increasing amounts of TNPPE. At comparable concentrations of TNPPE, small-angle X-ray diffraction profiles showed a broad scattering band, which obscured the sharp diffraction patterns. Taken together, these results probably indicate the segregation of anhydrous and unordered TNPPE-rich domains from a TNPPE-poor but ordered PE phase.

Apart from hexagonal (H_{II}) phase prefering PE systems, TNPPE also strongly influenced the macroscopic organization of the typical bilayer-forming PC. In agreement with the data

of Tilcock et al. (1982), 20 mol % DOPC was sufficient to stabilize the bilayer organization in DOPE up to 40 °C. From our experiments on PC/PE samples in which DOPE was partially replaced by DOTNPPE, we can conclude that TNPPE molecules show an even stronger tendency to destabilize a bilayer structure than PE. In mixtures of DOPC with a relatively high amount of DOTNPPE, the phase behavior is complex, as indicated by ^{31}P NMR measurements and by the detection of coexisting lamellar and hexagonal (H_{II}) phase and lipidic particles in freeze–fracture replicas. Apparently, these data demonstrate that even in the absence of DOPE the DOTNPPE molecules can give rise to hexagonal (H_{II}) phase formation. However, lower and biologically more relevant TNPPE concentrations did not induce a hexagonal (H_{II}) phase in mixtures with PC. Instead, the lipids were organized in closely packed lipidic particles, which may be interpreted as inverted micelles, possibly representing an intermediate stage between bilayer and hexagonal (H_{II}) phase (Verkleij, 1984; De Kruijff et al., 1980a).

In order to gain insight in the molecular origin of the bilayer-destabilizing capacity of TNPPE, it is useful to consider the various factors determining the polymorphic phase behavior of PE's, e.g., (i) acyl chain melting characteristics, (ii) molecular shape concept, and (iii) interbilayer attractive forces.

(i) The reorganization from bilayer to hexagonal (H_{II}) phase is a fluid–fluid transition that strongly depends on the fatty acid composition of the lipid. Both increasing unsaturation and increasing chain length result in a decreased bilayer to hexagonal (H_{II}) phase transition temperature (De Kruijff et al., 1984). It is most unlikely that the bilayer destabilizing effect of TNPPE can be understood in relation to fluidity since TNPPE does not shift the gel to liquid-crystalline phase transition temperature in hydrated mixtures with PE. Furthermore, in the experiments presented in this paper, the acyl chains of the different phospholipid classes in hydrated mixtures were identical.

(ii) The shape–structure model of Cullis & De Kruijff (1979) relates the overall dynamic molecular shape of a phospholipid to its macroscopic organization in aqueous dispersions. It should be noted that this shape concept is inclusive of the following factors: (1) geometrical space occupied by the isolated molecule, (2) intermolecular interactions, and (3) hydration properties of the lipid head groups. For PE as an example, it can be noticed that the ethanolamine head group is relatively small as compared the the cross-sectional area of the hydrocarbon chains and that the head groups can form intermolecular hydrogen bonds, thereby leading to a "cone" shape of the molecules, compatible with hexagonal (H_{II}) phase organization. Furthermore, it is known that reduced hydration of PE decreases the lamellar to hexagonal phase transition temperature (Luzzati, 1968; Seddon et al., 1983). In comparison to PE, the TNPPE head group occupies a larger area irrespective of its orientation. In addition, incorporation of the bulky TNPPE head group will disrupt the formation of hydrogen bonds between PE molecules. These properties of the trinitrophenyl derivative would suggest a more cylindrical shape and consequently a bilayer-stabilizing effect of the molecule. However, in contrast to PC and PE, the TNPPE head groups apparently do not bind water. Therefore, this dehydration property of TNPPE must be the most important factor, responsible for the pronounced bilayer destabilizing property of the molecule. This suggestion is reinforced by the finding that TNPPE incorporation in PE decreased the repeat distance in the hexagonal (H_{II}) phase, probably reflecting a reduced water content inside the tubes. This is in agreement with the observation of Seddon et al. (1984) that the long spacing of hexagonally organized PE decreases at lower water concentrations.

(iii) The formation of the hexagonal (H_{II}) phase has been suggested to be an interbilayer fusion process (Cullis et al., 1980). With respect to this phenomenon, the orientation of the TNPPE rings in hydrated mixtures with PC and/or PE is of importance. In relation to the hydrophobic character of the TNPPE molecule, two possibilities can be considered. First, the trinitrophenyl rings could be oriented along the interface, thereby reducing the mean hydration of the bilayer surface and consequently allowing the adjacent lamellae to come in close apposition. Second, the trinitrophenyl groups of TNPPE could be located in the aqueous phase, possibly oriented perpendicular with respect to the bilayer surface, in contrast to the polar head group of several "normal" phospholipids that are oriented parallel to the plane of the bilayer (Franks, 1976; Worchester & Franks, 1976; Büldt et al., 1978). Such a conformation of TNPPE was also suggested from monolayer studies at high surface pressure (Bishop et al., 1979). In combination with the proposed tendency for interbilayer ring–ring interaction, such an orientation would result in attractive forces between adjacent bilayers. Consequently, in both cases the interbilayer distance would decrease locally, resulting in inter bilayer fusion and hexagonal (H_{II}) phase formation. The required local dehydration of the bilayers emphasizes the exclusive role of the anhydrous TNPPE molecules in the formation of nonbilayer structures.

Finally, results obtained from hydrated microsomal phospholipid samples in which the aminophospholipids were trinitrophenylated suggest that TNBS can be a useful tool in studying the possible relation between the presence of nonbilayer structure preferring phospholipids in the microsomal membrane and functions of the endoplasmic reticulum. In contrast, since trinitrophenylation of PE dramatically influences the lipid phase behavior, results obtained from studies concerning the aminophospholipid asymmetry using TNBS [for a comparison, see Drenthe et al. (1980) vs. Miljanich et al. (1981)] should be used with caution.

In summary, the observations presented in this paper lead to the following conclusions. First, the TNPPE head group shows an anhydrous character. Second, TNPPE is to a limited extent soluble in hydrated PE. Third, in hydrated mixtures with PC and/or PE, the phosphate moiety of the TNPPE molecule undergoes long-axis rotation. Fourth, in these samples the TNPPE head groups show a difference in local order and/or motion as compared with those of PC and PE, possibly due to a reorientation of the trinitrophenyl rings. Finally, TNPPE destabilizes the bilayer organization in PC and/or PE, predominantly due to dehydration effects and trinitrophenyl ring–ring interactions.

ACKNOWLEDGMENTS

We thank Dr. B. Roelofsen for his generous gift of the phospholipase C. We gratefully acknowledge Dr. J. Moonen, W. S. M. Geurts van Kessel, and R. Dijkman for their technical advice and Leann Tilley for correcting the English.

Registry No. DETNPPE, 98874-81-8; DEPE, 19805-18-6; DOPC, 4235-95-4; DOPE, 4004-05-1; DOTNPPE, 98874-82-9.

REFERENCES

Bishop, D. G., Bevers, E. M., Van Meer, G., Op den Kamp, J. A. F., & Van Deenen, L. L. M. (1979) *Biochim. Biophys. Acta 551*, 122–128.

Bligh, E. G., & Dyer, W. J. (1959) *Can. J. Biochem. Physiol. 37*, 911–913.

Borle, F., & Seelig, J. (1983) *Biochim. Biophys. Acta 735*, 131–136.
Böttcher, C. J. F., Van Gent, C. M., & Pries, C. (1961) *Anal. Chim. Acta 24*, 203.
Broekhuyse, R. M. (1969) *Clin. Chim. Acta 23*, 457–461.
Büldt, G., Gally, H. U., Seelig, A., Seelig, J., & Zaccai, G. (1978) *Nature (London) 271*, 182–184.
Comfurius, P., & Zwaal, R. F. A. (1979) *Biochim. Biophys. Acta 488*, 36–42.
Cullis, P. R., & De Kruijff, B. (1976) *Biochim. Biophys. Acta 436*, 523–540.
Cullis, P. R., & De Kruijff, B. (1978) *Biochim. Biophys. Acta 513*, 31–42.
Cullis, P. R., & De Kruijff, B. (1979) *Biochim. Biophys. Acta 559*, 399–420.
Cullis, P. R., De Kruijff, B., & Richards, R. E. (1976) *Biochim. Biophys. Acta 426*, 433–466.
Cullis, P. R., De Kruijff, B., Hope, M. J., Nayar, R., & Schmid, S. L. (1980) *Can. J. Biochem. 58*, 1092–1100.
Dallner, G. (1974) *Methods Enzymol. 31*, 191–201.
De Kruijff, B., Van den Besselaar, A. M. H. P., Cullis, P. R., Van den Bosch, H., & Van Deenen, L. L. M. (1978) *Biochim. Biophys. Acta 514*, 1–8.
De Kruijff, B., Cullis, P. R., & Verkleij, A. J. (1980a) *Trends Biochem. Sci. (Pers. Ed.) 5*, 79–81.
De Kruijff, B., Morris, G. A., & Cullis, P. R. (1980b) *Biochim. Biophys. Acta 598*, 206–211.
De Kruijff, B., Rietveld, A., & Cullis, P. R. (1980c) *Biochim. Biophys. Acta 600*, 343–357.
De Kruijff, B., Cullis, P. R., Verkleij, A. J., Hope, M. J., Van Echteld, C. J. A., & Taraschi, T. F. (1984) in *The Enzymes of Biological Membranes* (Martinosi, A., Ed.) Plenum, New York.
Depierre, J. W., & Dallner, G. (1975) *Biochim. Biophys. Acta 415*, 411–472.
Diembeck, H., & Eibl, H. (1979) *Chem. Phys. Lipids 24*, 237–244.
Drenthe, E. H. S., Klompmakers, A. A., Bonting, S. L., & Daemen, F. J. M. (1980) *Biochim. Biophys. Acta 603*, 130–141.
Eibl, H. (1980) *Chem. Phys. Lipids 26*, 239–247.
Folch, J., Less, M., & Sloane Stanley, G. H. (1957) *J. Biol. Chem. 226*, 497–509.
Franks, N. P. (1976) *J. Mol. Biol. 100*, 345–358.
Higgins, J. A., & Pigott, C. A. (1982) *Biochim. Biophys. Acta 693*, 151–158.
Hoekstra, D., & Martin, O. C. (1982) *Biochemistry 21*, 6097–6103.
Hui, S. W., Stewart, T. P., Yeagle, P. L., & Albert, A. D. (1981) *Arch. Biochem. Biophys. 207*, 227–240.
Jiang, R. T., Shyy, Y.-J., & Tsai, M.-D. (1984) *Biochemistry 23*, 1661–1667.
Knoll, G., Oebel, G., & Plattner, H. (1982) *Protoplasma 111*, 161–176.
Kohler, S. J., & Klein, M. P. (1977) *Biochemistry 16*, 519–526.
Litman, B. J. (1974) *Biochemistry 13*, 2844–2848.
Litman, B. J. (1975) *Biochim. Biophys. Acta 413*, 157–162.
Lucy, J. A. (1964) *J. Theor. Biol. 7*, 360–375.
Luzzati, V. (1968) in *Biological Membranes* (Chapman, D., Ed.) Vol. 1, pp 71–123, Academic Press, London.
Luzzati, V., Reiss-Husson, F., Rivas, E., & Gulik-Krzywicki, T. (1966) *Ann. N.Y. Acad. Sci. 137*, 409–413.
Miljanich, G. P., Nemes, P. P., White, D. L., & Dratz, E. A. (1981) *J. Membr. Biol. 60*, 249–255.
Rand, R. P., Tinker, D. O., & Fast, P. G. (1971) *Chem. Phys. Lipids 6*, 333–342.
Rothman, J. E., & Kennedy, E. P. (1977) *J. Mol. Biol. 110*, 603–618.
Seddon, J. M., Cevc, G., & Marsh, D. (1983) *Biochemistry 22*, 1280–1289.
Seddon, J. M., Cevc, G., Kaye, R. D., & Marsh, D. (1984) *Biochemistry 23*, 2634–2644.
Seelig, J. (1978) *Biochim. Biophys. Acta 515*, 105–140.
Shipley, G. G. (1973) in *Biological Membranes* (Chapman, D., & Wallace, D. F. H., Eds.) Vol. 2, pp 1–89, Academic Press, London.
Siakotos, A. N. (1967) *Lipids, 2*, 87–88.
Sleight, R. G., & Pagano, R. E. (1983) *J. Biol. Chem. 258*, 9050–9058.
Söderman, O., Arvidson, G., Lindblom, G., & Fontell, K. (1983) *Eur. J. Biochem. 134*, 309–314.
Stier, A., Finch, S. A. E., & Bösterling, B. (1978) *FEBS Lett. 91*, 109–112.
Tilcock, C. P. S., Bally, M. B., Farren, S. B., & Cullis, P. R. (1982) *Biochemistry 21*, 4596–4602.
Ulminus, J., Wennerström, H., Lindblom, G., & Arvidson, G. (1977) *Biochemistry 16*, 5742–5745.
Van Deenen, L. L. M., & De Haas, G. H. (1964) *Adv. Lipid Res. 2*, 167–234.
Van Dijck, P. W. M., De Kruijff, B., Van Deenen, L. L. M., De Gier, J., & Demel, R. A. (1976) *Biochim. Biophys. Acta 455*, 576–587.
Van Duijn, G., Verkleij, A. J., & De Kruijff, B. (1984) *Biochemistry 23*, 4969–4977.
Van Echteld, C. J. A., Van Stigt, R., De Kruijff, B., Leunissen-Bijvelt, J., Verkleij, A. J., & De Gier, J. (1981) *Biochim. Biophys. Acta 648*, 287–291.
Vasilenko, I., De Kruijff, B., & Verkleij, A. J. (1982) *Biochim. Biophys. Acta 685*, 144–152.
Verkleij, A. J. (1984) *Biochim. Biophys. Acta 779*, 43–63.
Worcester, D. L., & Franks, N. P. (1976) *J. Mol. Biol. 100*, 359–378.